Assembling Mn:ZnSe Quantum Dots-siRNA Nanoplex for Gene Silencing in Tumor Cells

Journal:	*Biomaterials Science*
Manuscript ID:	BM-ART-08-2014-000306
Article Type:	Paper
Date Submitted by the Author:	19-Aug-2014

Complete List of Authors:	Wang, Yucheng; Nanyang Technological University, Yang, Chengbin; Nanyang Technological University, School of Electrical and Electronic Engineering Hu, Rui; Nanyang Technological University, School of Electrical and Electronic Engineering Toh, Hui Ting; Nanyang Technological University, Division of Structural Biology & Biochemistry, School of Biological Sciences Liu, Xin; Lawrence Berkeley National Laboratory, Lin, Guimiao; Shenzhen University, School of Medicine Yin, Feng; Nanyang Technological University, School of Electrical and Electronic Engineering Yoon, Ho Sup; Nanyang Technological University, Biology; Yong, Ken-Tye; Nanyang Technological University,

Assembling Mn:ZnSe Quantum Dots-siRNA Nanoplex for Gene Silencing in Tumor Cells

Yucheng Wang,[a] Chengbin Yang,[a] Rui Hu,[a] Hui Ting Toh,[b] Xin Liu,[c] Guimiao Lin,[d] Yin Feng,[a] Ho Sup Yoon[b,e] and Ken-Tye Yong[*a]

[a]School of Electrical and Electronic Engineering, Nanyang Technological University, Singapore 639798, Singapore; Email: ktyong@ntu.edu.sg
[b]Division of Structural Biology & Biochemistry, School of Biological Sciences, Nanyang Technological University, Singapore 639798, Singapore
[c]Department of Chemical and Biological Engineering, University at Buffalo (SUNY), Buffalo, New York 14260, United States
[d]The Engineering Lab of Synthetic Biology and the Key Lab of Biomedical Engineering, School of Medicine, Shenzhen University, Shenzhen, 518060, China
[e]Department of Genetic Engineering, College of Life Sciences, Kyung Hee University, Yongin-si Gyeonggi-do, 446-701, Republic of Korea

*Corresponding author: Ken-Tye Yong, PhD, School of Electrical and Electronic Engineering, Nanyang Technological University, Singapore 639798, Singapore Tel: +65-6790-5444, email: ktyong@ntu.edu.sg

Abstract:

In this work, we demonstrate the use of manganese doped zinc selenide QDs (Mn:ZnSe d-dots) for gene delivery *in vitro*. Specifically, the d-dots were prepared as nanoplex in facilitating the intracellular delivery of small interfering RNA (siRNA) molecules to the pancreatic cancer cells (Panc-1) thereby inducing sequence-specific silencing of the oncogenic K-Ras mutations in pancreatic carcinoma. For nanoplex preparation, a layer-by-layer (LBL) assembling method was adopted to modify the d-dots surface with cationic polymer poly(allylamine hydrochloride) (PAH) or Polyethylenimine (PEI) in generating positive surface potential for complexing with K-Ras siRNA molecules. Owing to the unique and stable PL properties of the d-dots, siRNA transfection and the subsequent intracellular release profile from the d-dot/polymer-siRNA nanoplexes were monitored by fluorescence imaging. Quantitative result from flow cytometry study suggested that high gene transfection efficiency was achieved. The expression of the mutant K-Ras mRNA in Panc-1 cells was observed to be significantly suppressed upon transfecting them with the nanoplexes formulation. More importantly, cell viability studies showed that the d-dot/PAH nanoplexes were biocompatible and non-toxic even at concentrations as high as 160 μg mL^{-1}. Furthermore, the amine-terminated surface could be further modified to obtain multiple bio-functions. Based on these results, we envision that the designed d-dot nanoplexe can be developed as a flexible nanoplatform for both fundamental and practical clinical research applications.

Key wards: Mn:ZnSe d-dots, pancreatic cancer, siRNA, gene therapy, toxicity

Introduction

Pancreatic cancer is one of the most common cancers with less than 5% of 5-year survival rate[1]. As this disease is extremely difficult to treat with conventional therapies, development of novel therapeutic approaches is urgently needed. Due to the advancement of cancer biology in the past few decades, RNA interference (RNAi), which is a sequence specific post-transcriptional gene silencing mechanism induced by double-stranded RNA (dsRNA), has been developed as a novel platform for gene therapy of disease[2]. Chemically synthesized small-interfering RNAs (siRNAs) can be delivered to tumor cells for initiating specific degradation of target messenger RNA (mRNA) of complementary sequence thereby inhibiting the expression of the corresponding cancer-promoting genes[2, 3]. However, the application of naked siRNA molecules is challenged by limited uptake efficiency and short half-life due to nuclease-mediated degradation[4]. Recently, viral vectors and synthetic materials, such as liposomes, peptide dendrimers, polymers and inorganic nanoparticles (e.g. noble metals, metal oxides, nanocarbons and mesoporous silica), have been investigated as potential carriers for gene delivery[5-14]. Among them, fluorescent QDs have been extensively investigated owing to their chemical stability and large surface area for loading of gene materials. Most importantly, because of their exceptional optical properties, such as broad excitation profile, tunable colour and high resistance to photobleaching[15-18], QDs-based nanocarriers can serve as a multifunctional delivery system as well as imaging probes for long-term tracking and monitoring of the siRNA transfection process *in situ.* This will allow one to investigate the gene silencing mechanism in details[19-21]. However, most of the reported QD-based gene vectors are developed by using cadmium-based QDs and their potential toxicity remains a major debating and unsettle issue for them to be translated for in vivo and clinical research. Some research groups have revealed the breakdown and degradation of QDs in biological systems[22-24]. The release of the cadmium ions from the

particle surface to the biological environment may induce severe acute toxic effects. Although several *in vitro* and *in vivo* studies have demonstrated that proper protective inorganic and organic coatings on QDs surface will significantly reduce the nanoparticle toxicity, long-term studies are still needed to understand the ultimate fate of the QDs *in vivo*[25, 26].

To overcome this challenge, in this study, we developed manganese doped zinc selenide QDs (Mn:ZnSe d-dots) as biocompatible nanocarriers for in vitro gene delivery. These Mn:ZnSe d-dots are more acceptable for real-life biomedical applications comparing to the traditional types of QDs that contains toxic heavy metals (e.g. CdSe, CdTe, PbS and PbSe)[27]. For genetic therapy of pancreatic cancers, we designed an siRNA sequence specifically targeting the mutant K-Ras gene with a point mutation at condon 12, which is present in approximately 90% of all types of pancreatic cancers and associated with increased cell proliferation and resistance to apoptosis[28-30]. Mn:ZnSe d-dots-siRNA nanoplexes were constructed for efficient loading and traceable delivery of the K-Ras siRNA into pancreatic cancer cells. Specifically, the d-dots surface were modified with cationic polymer poly(allylamine hydrochloride) (PAH) or polyethylenimine (PEI), and subsequently complexed with siRNA molecules in forming nanoplexes. The nanoplexes were colloidally stable for weeks and the photoluminescence from the d-dots were highly stable against photobleaching. The expression of the mutant K-Ras mRNA in Panc-1 cells was significantly suppressed upon transfecting them with the nanoplexes. More importantly, cell viability studies showed that the d-dot/PAH nanoplexes were biocompatible and non-toxic.

Experiment section

Material

Mn-doped ZnSe quantum dots (Mn:ZnSe d-dots) were obtained from NN-labs and stored at 4 °C in dark. The as-received QDs (1mg mL^{-1} in water) were stabilized by mercaptopropinic acid (MPA) and dispersed in water. 1-Ethyl-3-(3-dimethylaminopropyl)carbodiimide (EDC), Poly(allylamine hydrochloride) (PAH, Mw =15 kDa), Polyethylenimine (PEI, Mw=1.8 kDa) and folic acid were purchased from Sigma-Aldrich. FAM-labeled small interference RNA (K-Ras $siRNA^{FAM}$, sense strand: 5'-FAM-GUUGGAGCU***GAU***GGCGUAGUU-3';
Antisense: 5' CUACGCC***AUC***AGCUCCAACUU-3', italic bold indicates the K-Ras mutation site) were purchased from Shanghai GenePharma (China). 18.2 MΩ·cm ultrapure water was used throughout the experiments.

Preparation of QD-based siRNA vector

The d-dots were developed as siRNA vectors through the Layer-by-Layer (LbL) assembly method. Cationic polyelectrolyte PAH was employed to modify the surface potential of the dots. 50 µl of d-dots stock solution (1mg mL^{-1}) was washed with ethanol and centrifuged at 10,000 rpm. Next, 250 µl of PAH solution of different concentration (0.05~10 mg mL^{-1}, in DI water) was added to re-disperse the d-dots precipitate, followed by short sonication and vortex for 20 min. After that, the d-dot/$PAH_{0.05\sim10}$ particles were collected by centrifugation at 15,000 rpm for 10 min to remove the non-adsorbed PAH. The resulting d-dot/PAH particles were dispersed in 200 µl of DEPC-treated water while aggregates were removed by centrifugation at 2000 rpm for 1 min. For siRNA loading, 100 µl of 10 µM K-Ras $siRNA^{FAM}$ solution was then introduced to the d-dot/PAH particles dispersion with gentle vortex and left undisturbed for 40 min. Subsequently, the d-dot/PAH/$siRNA^{FAM}$ complex was further incubated with 8 µl of PAH solution (1 mg mL^{-1}, in DI water) for 1h to form d-dot/PAH/$siRNA^{FAM}$/PAH nanoplexes. Centrifugation was used to further remove the excess PAH from the nanoplexes dispersion. The nanoplexes were redispersed in 100 ul of DEPC-treated water for cell transfection experiments. In a parallel experiment, PEI, a frequently reported polymeric gene transfecting material, was employed to form d-dot/PEI nanoplexes. To serve as a reference for d-dot/PAH, the d-dot/PEI nanoplexes were prepared following the same preparation method.

Preparation of folic acid conjugated nanoplexes

Covalent conjugation of the d-dot/PAH nanoplexes with folic acid (FA) was conducted using the standard EDC/NHS condensation method. Firstly, 1.5 mg of FA was dissolved in 2 mL PBS (pH 7.4), followed by mixing with 200 µL EDC (0.1 M in PBS) and 200 µL of NHS (0.2 M in PBS) for 1 h, allowing the carboxyl groups of FA being activated. Subsequently, 250 µl nanoplexes solution was added and the mixture was gently stirred at room temperature for 2 hours. The FA-conjugated nanoplexes were obtained by centrifugation and washed with PBS for 3 times to remove unreacted chemicals.

Nanoparticle characterizations

The UV-visible absorption spectra were obtained from a spectrophotometer (Shimadzu UV-2450). Photoluminescence (PL) spectra and lifetime were collected using a Fluorolog-3 spectrofluorometer. Quantum yields (QYs) of the Mn:ZnSe QD was determined by comparing the integrated emission of diluted d-dots to CdSe QDs with matched absorbance. The QY of the CdSe reference sample was calibrated by rhodamine 6G. The hydrodynamic size distribution profile and the zeta potential of the nanoparticle formulation were measured by a particle size analyzer system (90Plus, Brookhaven Instruments). Fourier transform infrared (FT-IR) spectra were measured by a Shimadzu FT-IR spectrometer. All measurements were performed at room temperature.

SiRNA transfection and gene expression analysis study

Panc-1 (ATCC® CRL-1469™) were cultured in Dulbecco's modified Eagle's medium (DMEM), supplemented with 10% fetal bovine serum (FBS, Hyclone), 100 μg mL^{-1} penicillin (Gibco) and 100 μg mL^{-1} streptomycin (Gibco). Cells were cultured at 37°C in a humidified atmosphere with 5% CO_2. Panc-1 cells were seeded in 6-well plates to approximately 30% cell confluence, and the culture medium was replaced with DMEM prior treatment. D-dot/PAH (PEI)-$siRNA^{FAM}$ nanoplexes dispersion was then added to the cell plates to give a final incubation concentration of the nanoplexes around 10 μg mL^{-1}. After 4 h incubation at 37 °C in humidified atmosphere with 5% CO_2, the cells were washed with PBS for three times and harvested for transfection efficiency determination. The cellular uptake efficiency was quantitatively evaluated by using a FACS Calibur flow cytometer (Becton Dickinson, Mississauga, CA). For gene expression analysis at 48 h post-transfection, the treated cells were continuously cultured in DMEM with 10% FBS. The cells were harvested and washed by PBS. The total RNA was extracted using TRIzol reagent (Invitrogen) and quantitated by a spectrophotometer (Nano-Drop ND-1000). After that, RNA was reverse transcribed to cDNA using the reagent kit from Promega according to the vendor's instructions. Real time quantitative RT-PCR was then carried out for the analysis of K-Ras relative mRNA expression by normalizing against the expression of Glyceraldehyde-3-phosphate dehydrogenase (GAPDH), which is one of the most commonly used housekeeping genes for gene expression comparisons. Forward and reverse primers used in real time RT-PCR were 5'-AGAGTGCCTTGACGATACAGC-3', 5'-ACAAAGAAAGCCCTCCCCAGT-3' for K-Ras mRNA, and 5'-ACCACAGTCCATGCCATCAC-3', 5'-TCCACCACCCTGTTGCTGTA-3' for GAPDH, respectively. In a parallel experiment, d-dot/PAH complex and free $siRNA^{FAM}$ with the same dosage level were introduced as negative controls while commercial transfection reagent Oligofectamine™ (Invitrogen) coupled $siRNA^{FAM}$ was used as positive control.

Cell viability evaluation

Cell viability was measured by the MTT (3-(4,5-dimethylthiazol-2-yl)-2, 5 diphenyltetrazolium bromide) assays. Toxic effects of the d-dot nanocarriers were tested on different cell lines, including two human pancreatic cancer cell lines (Panc-1 and Miapaca-2), human breast cancer cells (MDA-MB-231) and mouse leukaemic monocyte macrophage cells (RAW 264.7). The cells were seeded in a 96-well plate at a density of 5000 cells/well and incubated with different concentrations of d-dot/PAH nanoplexes for 48 h. In parallel experiment, different types of particles (i.e. d-dot, CdTe and CdTe/ZnS QDs, d-dot/PEI nanoplexes and d-dot/PAH-FA) were tested on RAW 264.7 macrophage cell line and biocompatibility of these particles were compared at the same dosage addition. In each assay, 20 μl of 5 mg mL^{-1} MTT in PBS was added and the cells were incubated for 4 h. 150 μl of 100% dimethylsulfoxide (DMSO, Sigma) was then added to dissolve the precipitate with 5 min gentle shaking. Absorbance was then measured with a microplate reader (Bio-Rad) at the wavelength of 490 nm. The cell viability was calculated as the ratio of the absorbance of the sample well to that of the control well and expressed as a percentage, assigning the viability of non-treated cells as 100%.

Results and discussions

Figure 1a shows the absorption and photoluminescent (PL) spectra of the MPA-stabilized Mn:ZnSe d-dots dispersion in water. The d-dots exhibit an absorption peak at 400 nm and a dopant emission peak at 590 nm with an FWHM (full width at half maximum) of 70 nm. Instead of band-edge transition in the host ZnSe matrix, the photogenerated exciton transfers energy into excited dopant states [31], which resulted in a large Stokes shift of ~190 nm. This is desirable for biomedical imaging applications as it helps to minimize the self-absorption of the d-dots and allows one to easily differentiate them from the background autofluorescence of biological samples[32]. The PL quantum yield (QY) of the d-dots is estimated to be around 20%. The PL decay curve could be fitted with a single exponential function with an estimated lifetime of τ=0.11 ms (Fig. 1b). This long luminescent lifetime in millisecond scale is consistent with literature reports [33], distinguishing the d-dots from common fluorescent QDs, as the optical transition in Mn^{2+} centre ($^4T_1$-$^6A_1$) is spin-forbidden. Figure 1c shows the hydrodynamic size distribution of the d-dots characterized by dynamic light scattering (DLS). The d-dots have a narrow size distribution with an average value of 11 nm. In addition, they have a negatively charged surface with a zeta potential value of -17 mV, owing to the carboxylic groups present on their surface. Figure. 1d shows the TEM image of the d-dots. The particles are crystalline and they have an average diameter of around 10 nm.

The d-dots were developed as siRNA vectors through a Layer-by-Layer (LbL) assembly method. Scheme. 1 illustrates the preparation steps, where cationic polymer poly(allylamine hydrochloride) (PAH) was employed for complexing with K-Ras siRNA molecules through electrostatic absorption. As compared to some other polymeric transfecting materials, such as PDDAC, and PAMAM dendrimers, which have been reported with acute in vitro toxic effects, the PAH polymer could be more feasible for in vivo applications owing to its biocompatibility [7]. It is worth noting that, by varying PAH concentration (Fig. 2), the d-dot/PAH clusters can be prepared with varying hydrodynamic sizes (47~200 nm), and the surface zeta-potential was also tunable over a wide range (+20~+48 mV). In addition, agarose gel electrophoresis was used to examine the loading of siRNA molecules onto d-dot/PAH particles (Fig. S1, Electronic Supplementary Information). The results suggest that the

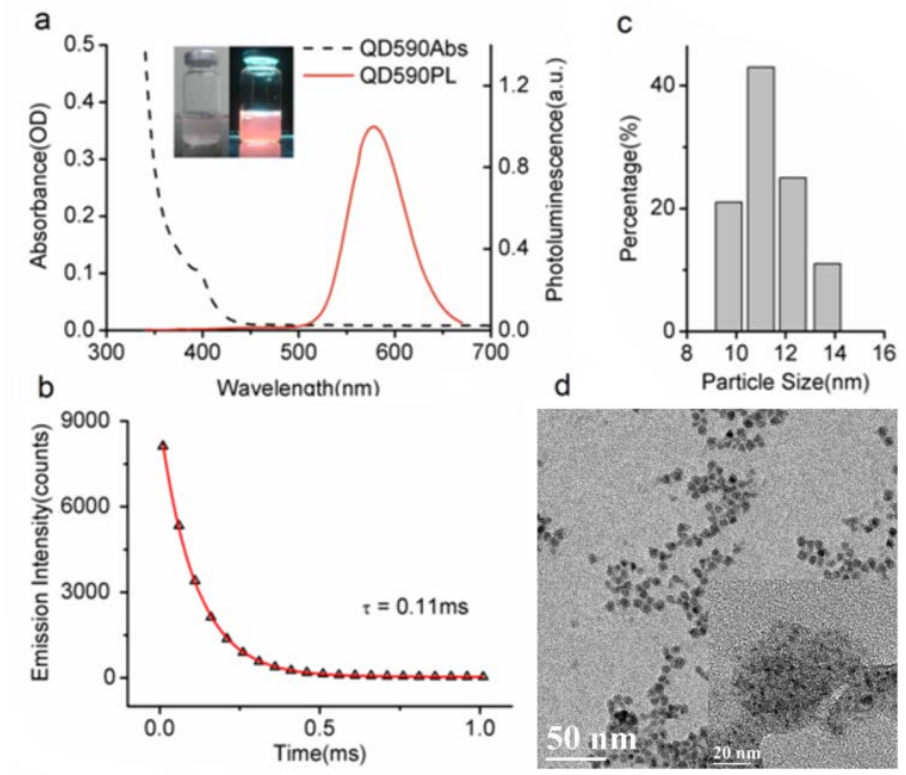

Figure. 1 (a) absorption and PL spectra of the Mn:ZnSe d-dots. (b) time-resolved PL decays of 590-nm-emitting d-dots. (c) DLS measurement of MPA-stabilized d-dots in de-ionized water. (d) TEM image of the d-dots. Inset is TEM image of the d-dot/PAH clusters.

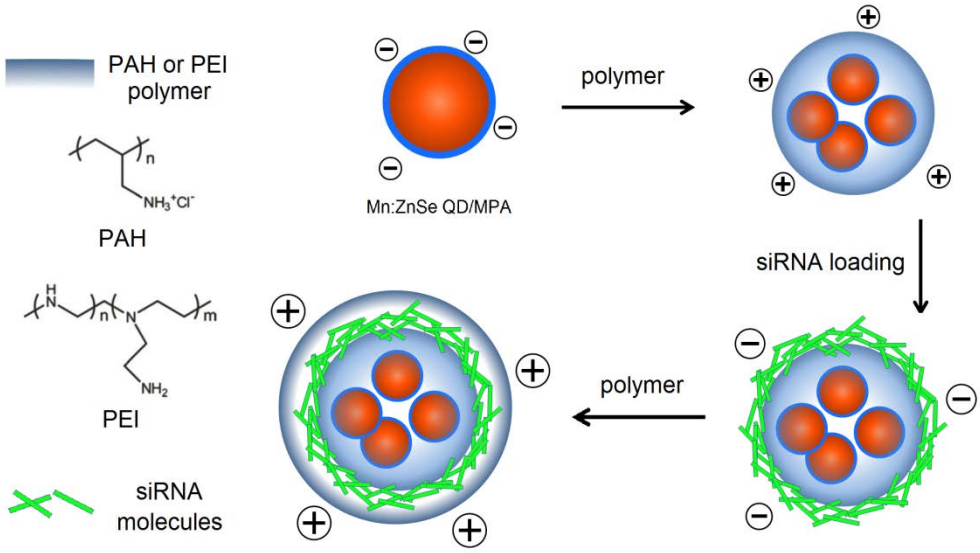

Scheme. 1 Schematic illustration of preparation steps of the Mn:ZnSe QDs based siRNA vectors.

d-dots without PAH coating cannot absorb negatively charged siRNA, while higher loading efficiency was observed for d-dot/PAH cluster with higher zeta potential. In a parallel experiment, d-dot/PEI nanoplexes prepared under same conditions exhibit higher zeta potential (+35~+58mV) than d-dot/PAH. The higher charge density of PEI can be more beneficial for loading of the oppositely charged gene material. After siRNA loading, a second PAH coating layer was applied, generating a surface with positive charges (~+30 mV). Because of the primary amine groups present by PAH, the capping layer can promote cellular uptake or provide anchor moieties for further modification with functional molecules. In Fig. 3, we monitored the hydrodynamic size and zeta potential changes of the particles during LbL assembly. The surface charge reversals clearly indicated deposition of alternating layers of the positively charged PAH and negatively charged siRNAs. It is noticeable that hydrodynamic size of

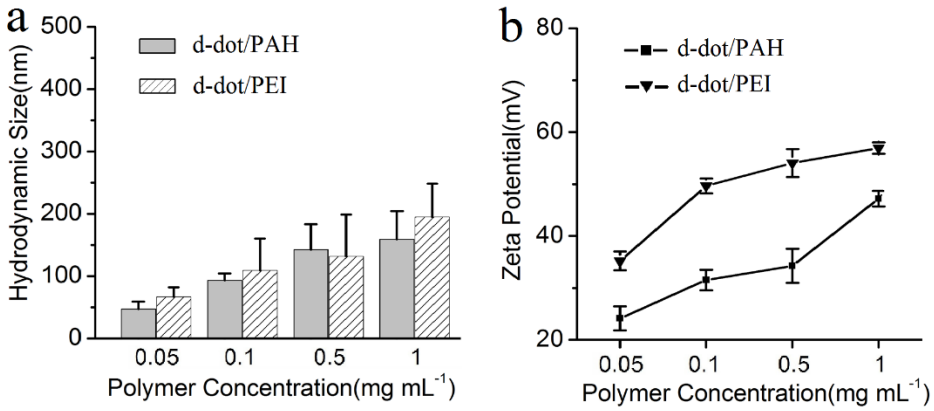

Figure. 2 (a) Hydrodynamic size and (b) surface zeta potential of the d-dot/PAH and d-dot/PEI clusters prepared using polymer solution of different concentrations.

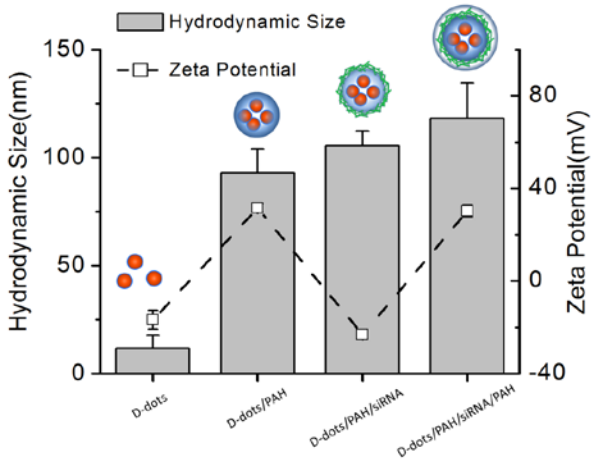

Figure. 3 Monitoring of the change in particle hydrodynamic size and zeta potential during the LBL construction steps to prepare d-dot/PAH0.1/siRNAFAM/PAH nanoplexes.

the particles increases dramatically after coating of the first PAH layer. This observation, together with the TEM image (Fig. 1d, inset), indicate that multiple d-dots have been co-encapsulated to form a relatively large d-dot/PAH cluster. The hydrodynamic size change of the as-produced nanoplex formulations was monitored over a period of 2 weeks (Fig. S2). Result suggests that the nanoplex possesses an excellent colloidal stability.

As shown in Fig. S3, we investigate the PL property of the prepared d-dot/PAH-siRNA^{FAM} nanoplexes, while PL spectra of d-dot/PAH and free siRNA^{FAM} are also presented for comparison. The assembly of the nanoplex does not affect the characteristic peak wavelengths and fluorescence resonance energy transfer (FRET) between the d-dots and FAM was not observed. This is quite different from the red emitting CdSe QD previously reported for gene release monitoring [19]. For multichannel imaging purpose, narrow band-pass filter are normally employed to avoid crosstalk between adjacent channels, while PL bandwidth of the fluorescent labels are requested to be narrow. In our case, crosstalk between the FAM labels (520 nm) and d-dots (590 nm) signals was fundamentally avoided by employing different excitation wavelengths (i.e., UV for d-dot and blue light for FAM), because neither of the excitations can activate the two labels simultaneously. More importantly, owing to the large Stokes shift of the d-dots, light source for FAM excitation can be selected over a wide wavelength range between 400 and 500 nm without activating the d-dots. In view of this, d-dot shows an advantage over conventional band-edge emitting QD, as it may simplify the requirements for the optical system and provide a chance to include more optical channels. Additionally, the photostablity of the nanoplex was also investigated. Fluorescent images shown in Fig. S4 suggest that, compared with FAM fluorophores, the inorganic d-dots are more suitable probes for long term optical tracing owning to their high resistance against photobleaching.

The d-dot/PAH nanoplexes formulation was applied to deliver siRNAs that target the mutant oncogenic K-Ras gene in pancreatic cancer cells. In Fig. 4a, the successful delivery of the siRNAs can be easily identified through the green fluorescence from the FAM label at 4 h post transfection. Similar results were also observed in d-dot/PEI-siRNA^{FAM} treated cells (Fig. S5) and the positive control group using commercially available transfection reagent Oligofectamine™. As a comparison, there is no fluorescent signal in the cells treated with free siRNAs, suggesting that the naked siRNAs are not able to penetrate the cell membrane without the assistance of transfection agents. More interestingly, the overlay of the FAM and the d-dots channels shows both co-localization (yellow, a merge of green and red) and delocalization within the d-dot/polymer-siRNA^{FAM} treated cells. This indicates that the siRNAs were slowly released from the d-dots nanoplex surface. By further monitoring cells for 72 h post transfection, a variation in the intracellular distribution of d-dots can be observed (Fig. 4b). Furthermore, unlike Oligofectamine™ formulation, where no FAM signals was detected at 72 h post transfection, the FAM fluorescent

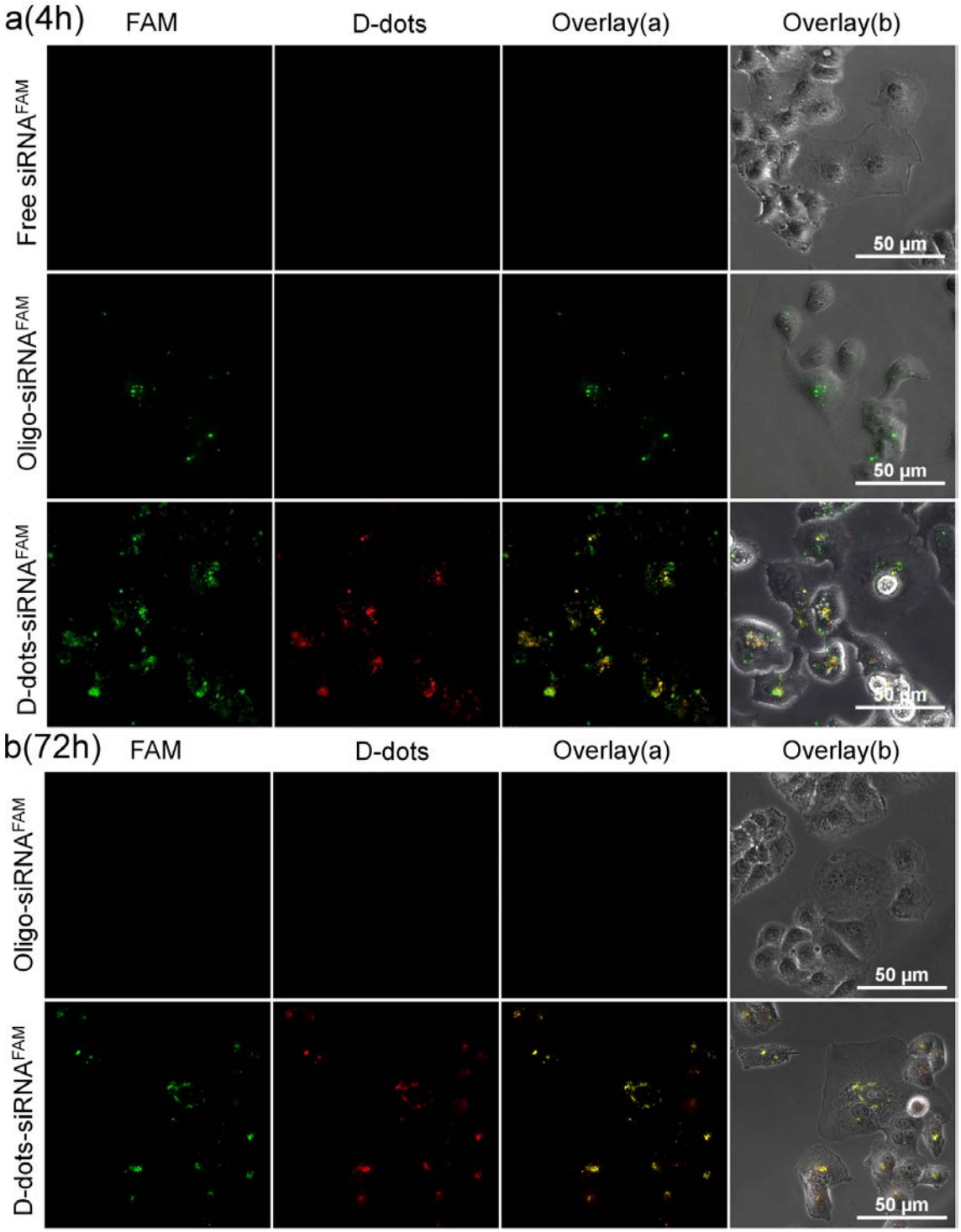

Figure. 4 (a), fluorescent image of Panc-1 cells treated with (i), free siRNAFAM, (ii), Oligo-siRNAFAM, and (iii), d-dot/PAH-siRNAFAM for 4 hours. (b) After 4 hours transfection with (iv), Oligo-siRNAFAM and (v) d-dot/PAH-siRNAFAM, the Panc-1 cells were further incubated in DMEM, and the images were taken at 72 hours post-transfection.

signals remained visible in the cells transfected by the d-dot/polymer nanoplexes (Fig. 4b and Fig. S4). This suggests that a fraction of siRNA^{FAM} molecules that are tightly bound to the d-dot/PAH (PEI) cluster surface have survived from degradation process within cells, and they may need longer time to be released to the cytoplasm. Cationic polymer coating plays an essential role in siRNA loading and release kinetics. Insufficient coating will result in less positively charged nanoplex and relatively weak siRNA surface binding. On the contrary, a higher siRNA loading efficiency can be achieved by using thicker polymer coating layer. However, this approach will cause a decrease in the siRNA release rate since the siRNA will be tightly bound by the strong electrostatic force. This

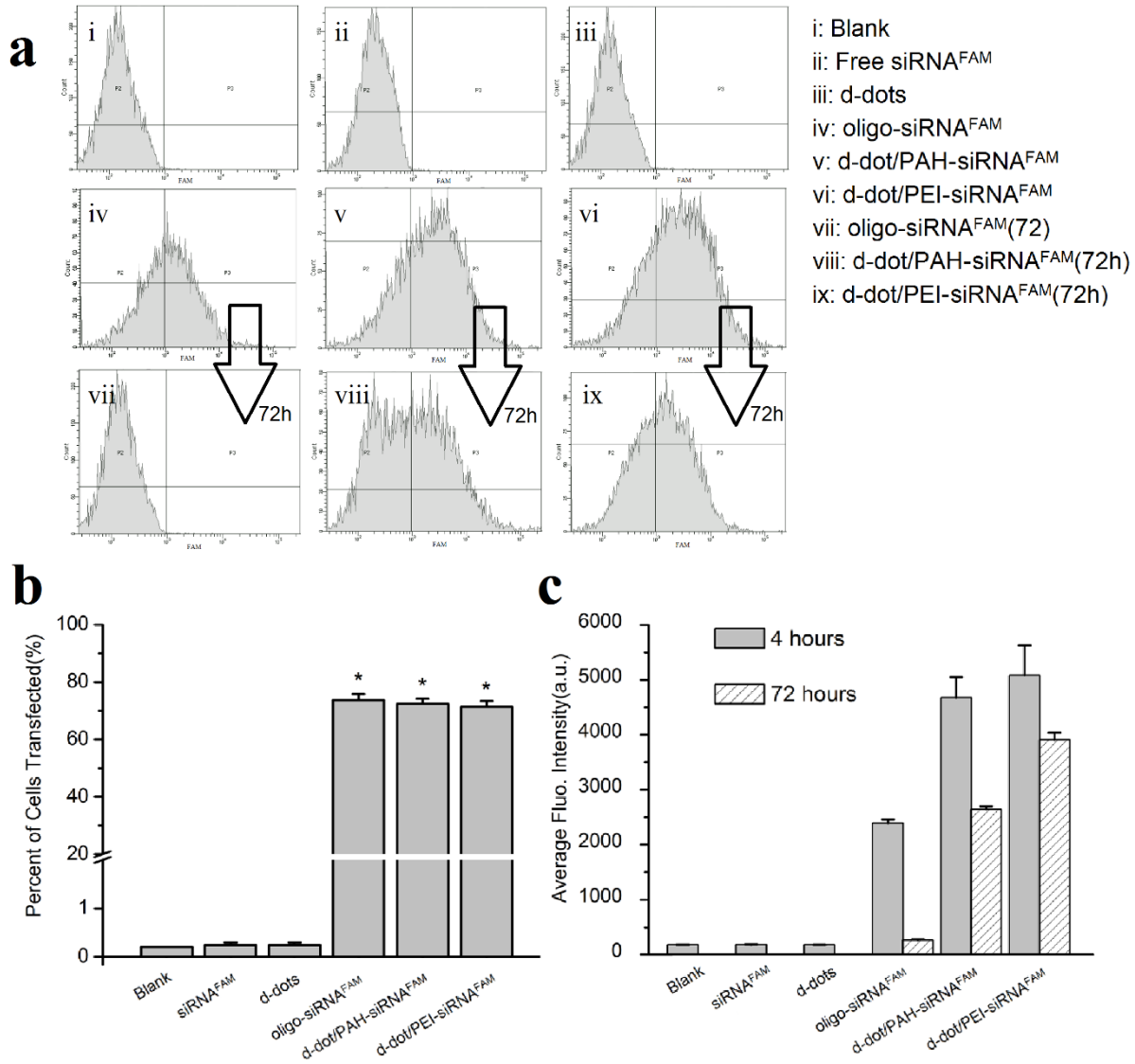

Figure. 5 Transfection efficiency of Panc-1 cells determined by flow cytometry analysis. (A), Representative pictures, where cells were treated with (i) blank, (ii) free siRNA^{FAM}, (iii) d-dot/PAH, (iv) Oligo-siRNA^{FAM} (v) d-dot/PAH-siRNA^{FAM} and (vi) d-dot/PEI-siRNA^{FAM} for 4 hours. (vii), (viii) and (ix) were collected at 72hours post-transfection, corresponding to (iv), (v) and (vi), respectively. (B), percentage of cells transfected after 4 h treatment, evaluated from experiments shown in (A). Values are means ± SD, n = 3. *, P < 0.005 vs blank, siRNA and d-dots. (C), average FAM fluoresence intensity of the treated cells (4- and 72 hours post-transfection) counted from experiments shown in (A).

situation will certainly influence the therapeutic activity of the nanoplex formulation. Our results suggest that a zeta potential between +20 mV and +40 mV is an optimum range for the nanoplex to successfully and effectively deliver siRNAs to the cells.

The transfection efficiency of the siRNAs into Panc-1 cells was quantitatively evaluated by flow cytometry analysis. Figure 5a shows the representative plots of the FAM intensity in cells treated with different formulations. After 4 hours incubation, comparable transfection efficiencies of 73.7%, 72.3% and 71.3% were observed for cells transfected by Oligo agent, d-dot/PAH and d-dot/PEI nanoplexes, respectively (Fig. 5B). These results are consistent with the fluorescent imaging analysis, indicating considerable accumulation of siRNAs inside the cells. On the contrary, no evident FAM signal was detected for the cases of free siRNA^{FAM}, d-dot nanoplexes only and blank cell groups. Figure 5C shows the average fluorescence intensity per cell count recorded in the flow cytometry evaluation. Because the average FAM intensity from the d-dot/PAH and d-dot/PEI treatment groups is two times higher than that of Oligo-siRNA^{FAM}, we consider that siRNA transfection by the two d-dot formulations is more effective. It is also noticeable that, after 72 hours of incubation, fluorescence signals almost disappeared in Oligo transfected cells (Fig. 5A and C). In contrast, around 56% and 77% of intensity still remained for d-dot/PAH and d-dot/PEI transfected cells. These observations are in accordance with our imaging results (Fig. 4b and Fig. S4), suggesting the protection and the partial release of siRNAs inside the cells.

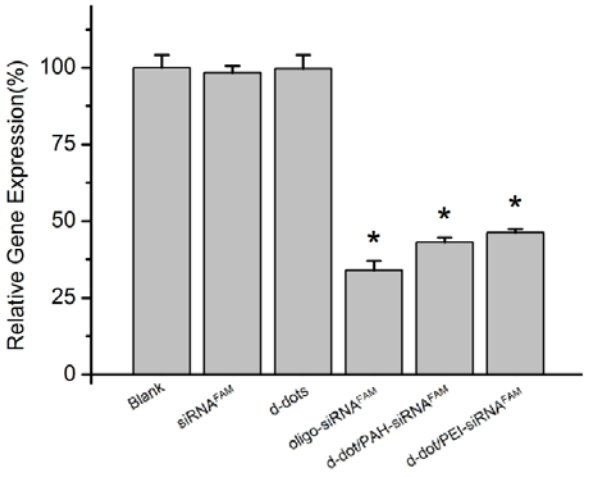

Figure. 6 K-Ras mRNA relative expression levels in Panc-1 cells were detected by real time quantitative RT-PCR. (a), Blank, (b), Free siRNA, (c), d-dots, (d), Oligo-siRNA, (e), d-dot/PAH-siRNA and (f), d-dot/PEI-siRNA complexes. Data are presented as means ± SD, n = 3. *, P < 0.005 vs blank, siRNA and d-dots.

Regulated expression of the targeted mRNA, regarded as the direct proof of successful RNAi process, was carried out to evaluate the therapeutic capability of the nanoplex formulation. Figure 6 shows the relative expression levels of mutant K-Ras mRNA in Panc-1 cells treated with different formulations after 72 hours of transfection. No evident differences in the expression levels were observed in the cells treated with d-dot/polymer complexes only or free siRNAs. In contrast, the expression level of the mutant K-Ras mRNA in cells transfected by Oligo-siRNA and d-dot/PAH-siRNA was found to be significantly suppressed to 34% and 43%, respectively. In comparison with d-dot/PAH, the silencing effect was not further promoted by using d-dot/PEI (46%), although it induced higher transfection efficiency. These results, together with the residual FAM intensity detected by flow cytometry at 72 h post-transfection, imply that d-dot/PAH complex with lower zeta potential could be more favourable than d-dot/PEI for gene release. Considering zeta potential of the d-dot complex is essential for siRNA binding and the value of d-dot/polymer is tunable over a wide range, the release kinetics of siRNA should be optimized in the future to obtain improved knockdown efficiency or sustained release for long term gene treatment.

MTT assays were conducted to evaluate the cytotoxicity of d-dots and d-dot/polymer complexes. As shown in Fig. 7a, in addition to the d-dots, cytotoxicity evaluation for MPA stabilized CdTe and CdTe/ZnS core/shell QDs, which have similar physical and optical properties, were also performed in this study as positive controls. The test was firstly conducted using macrophage cell line (RAW 264.7). Because macrophage cells internalized foreign particles nonspecifically through the phagocytosis process, the cytotoxicity evaluation could be less sensitive towards the discrepancy in internalization/accumulation rate of the particles with different surface modifications. At 48 h post treatment, CdTe QDs without ZnS shell capping exhibit severe toxicity. The 50% cell viability (IC50) was determined to be less than 10 μg mL^{-1}. Comparatively, ZnS capped CdTe QDs were found to be less toxic. The IC50 was greatly improved to above 40 μg mL^{-1} although the influence of the particles on cell viability was still pronounced, especially at high dosage concentrations. ZnS capping layer may protect the Cd-core from fast degradation, however, it cannot prevent the release of heavy metal ions to the biological environment especially when the QDs are exposed to intracellular oxidative conditions. On the contrary, after 48 h of incubation with d-dots, viability of the treated cells were maintained over 90% for concentrations as high as 160 μg mL^{-1}. These results indicate that the d-dots are highly biocompatible. Furthermore, viabilities of the RAW 264.7 cells treated with d-dot/polymer nanoplexes was shown in Fig. 7b. It is

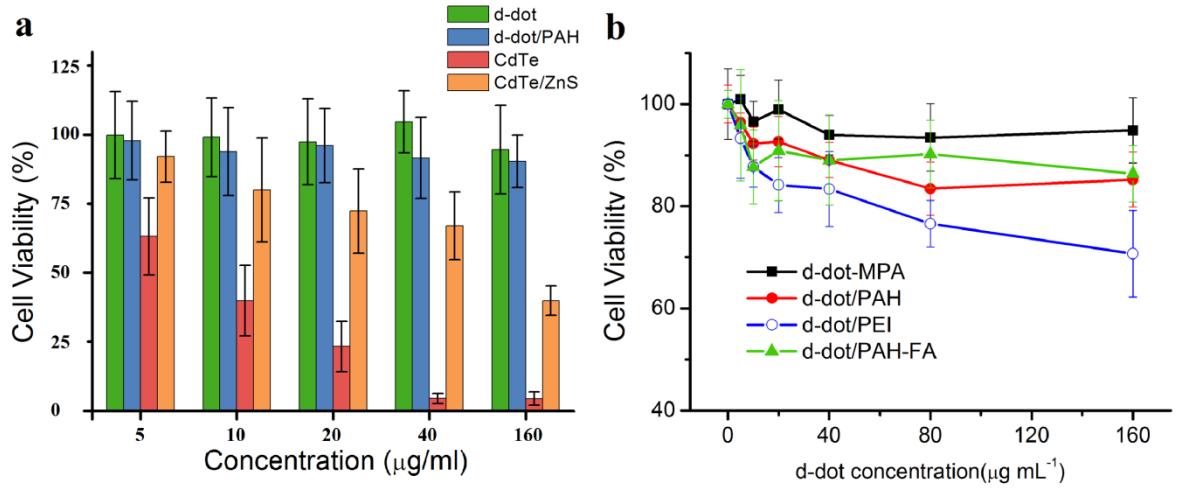

Figure. 7 (a), Cytotoxicity tests of four types of nanoparticles, i.e. d-dots, PAH-coated d-dots, CdTe QDs and CdTe/ZnS core/shell QDs. RAW 264.7 cells were treated with different concentrations of the particles for 48 hours. The particles were MPA-stabilized except for d-dot/PAH complex. (b), Cytotoxicity tests of the d-dot/polymer nanocomplexes and d-dot/PAH-FA. Data for d-dot/MPA was presented as reference.

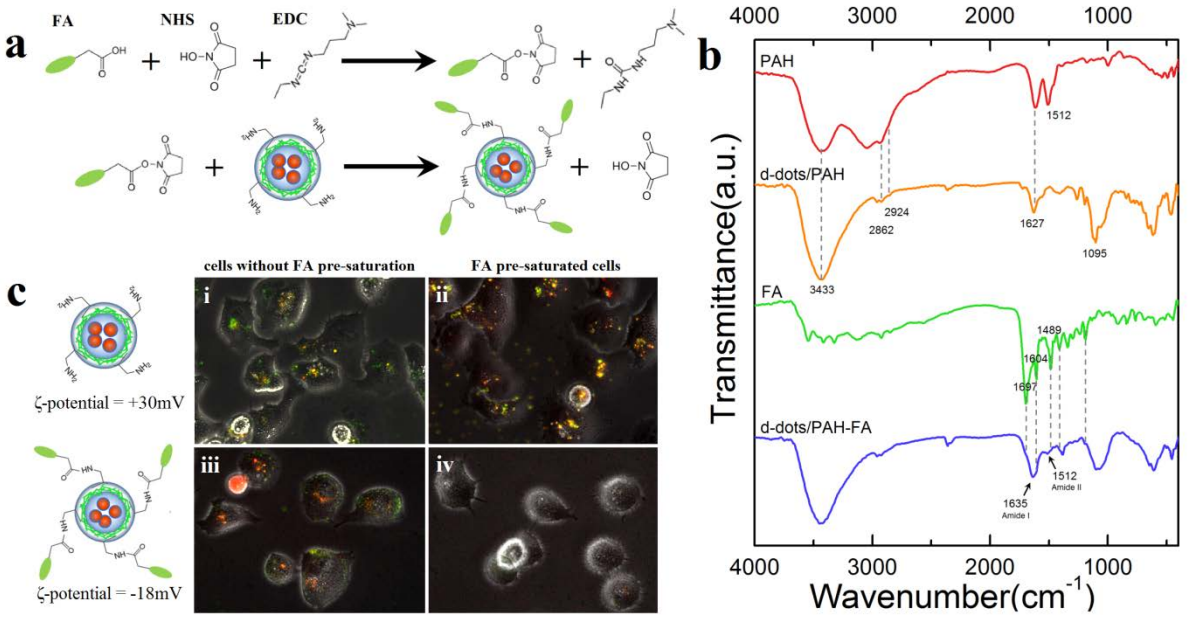

Figure. 8 (a), schematic illustration of the method to prepare FA conjugated d-dot/PAH nanoplexes. (b), FT-IR spectra of PAH, d-dot/PAH, folic acid and d-dot/PAH-FA nanocomposites. (c), fluorescence image of Panc-1 cells treated with unconjugated (i, ii) and FA-conjugated (iii, iv) nanoplexes. The cells in (ii) and (iv) were pre-saturatured with free FA before incubation with the nanocomposites.

observable that toxicity of the d-dot nanoplexes was mainly determined by the polymer coating, rather than the inorganic d-dots. In comparison with d-dot/PEI reference group, higher viabilities were evaluated for cells treated with equal amount of d-dot/PAH nanoplex. To further confirm the biocompatibility of the d-dot/PAH, we investigated the toxic effects of the d-dot/PAH complexes on different cell lines, including human breast cancer cells (MDA-MB-231) and two human pancreatic cancer cell lines (Panc-1 and Mia PaCa-2). At 48 hours after exposure, all the four cell lines maintained over 80% viability across a wide range of dosages up to 160 μg mL^{-1} (Figure S6). These results suggested that the as-prepared d-dot/PAH complexes (~+30 mV) are highly biocompatible and will be a promising optical contrast agent for biomedical applications ranging from imaging to drug delivery.

Because PAH polymer exhibits plenty of primary amino groups, which can serve as anchor moieties to conjugate with different functional molecules, the d-dot complexes capped with a second PAH layer could be further modified to receive multiple bio-functions. For example, we conjugated folic acid (FA) on the d-dot/PAH to obtain ability for cancer cell targeted gene delivery. Figure 8a schematically illustrates the preparation of folic acid conjugated nanoplexes, where EDC/NHS condensation method was applied for crosslinking. According to our results, after conjugation with FA, zeta potential of the nanoplex changed from +30 mV to a negative value (-18 mV). Compared with positive charges, a negatively charged surface helps to reduce non-specific internalization of the particle by cells [34]. MTT results shown in Fig. 7b confirm the biocompatibility of these d-dot/PAH-FA formulations. Surface characterization of the FA conjugated d-dot/PAH were studied by using FT-IR spectroscopy. For comparison, spectra of PAH, d-dot/PAH, FA and d-dot/PAH-FA are shown in Fig. 8b. The d-dot/PAH complexes exhibit characteristic peaks of amine group in PAH polymer including N-H stretching mode at 3433 cm^{-1} and NH_2 deformation vibration at 1627 cm^{-1}. Appearance of the two bands at 2924 and 2862 cm^{-1} corresponded to asymmetric and symmetric stretching vibration of $-CH_2$, respectively. Compared with PAH polymer in hydrochloride form, the NH_3^+ deformation vibration at 1512 cm^{-1} disappeared in d-dot/PAH after forming the complexes, accompanying with presence of a new band at 1095 cm^{-1} which is assigned to C-N stretching mode. Conjugation of folic acid onto d-dot/PAH was substantiated by the emergence of amide I band at 1635 cm^{-1} and amide II band at 1512 cm^{-1}, which were attributed to C=O stretch and NH deformation in the secondary amides, respectively. Meanwhile, a series of characteristic IR absorption peaks of FA located at 1697 cm^{-1} (carboxyl), 1605 cm^{-1} (benzene), and 1481cm^{-1} (hetero-ring) were also visible in the spectra of d-dot/PAH-FA. All these results substantiated that the folic acid molecules were successfully conjugated on d-dot/PAH surface.

To demonstrate the ability of the d-dot/PAH-FA for cancer cell targeted siRNA delivery, fluorescent images of Panc-1 cells treated with non-conjugated and FA-conjugated complexes are compared in Fig. 8c. Prior to transfections, Panc-1 cells in (ii) and (iv) were pre-saturated with free folic acid to block FA receptors (FAR) available on cell surface. As shown in the fluorescent images, Panc-1 cells were stained with FA conjugated nanoplexes after 2 hours incubation (iii), whereas minimal signal was observed from cells pre-saturated with FA (iv). These results suggested that uptake of the particles involve the interaction between FA and FAR. On the contrary, for

unconjugated nanoplexes, accumulations of the particles were observed in both unsaturated and FAR-blocked cells suggesting the non-specific nature of the uptake due to the positive surface charges. Considering the FAR is overexpressed on many human cancer cell lines, these results indicated that the particles can be functionalized with folic acid for cancer cell targeted gene delivery. More importantly, these results exemplified that the amine groups present on the second PAH layer could be employed to link with molecules to obtain multiple bio-functions. For example, to explore the applications for in vivo gene delivery and tumor therapy, PEG should be conjugated for improved stability in serum and prolonged circulation time of the particles after intravascular administration[35].

Conclusions

In summary, we have developed Mn:ZnSe d-dot as a biocompatible nanocarrier for gene delivery in vitro. Using d-dot/polymer nanoplex as transfection agent, siRNAs targeting the mutant oncogenic K-Ras gene were delivered into pancreatic cancer cells for sequent specific gene therapy. Owing to unique and stable PL properties of the d-dots, the delivery of siRNA and the subsequent intracellular release from the d-dot/polymer-siRNA nanoplexes can be monitored by fluorescence imaging. Quantitative result from flow cytometry study suggested that high gene transfection efficiency was achieved with the use of the prepared nanoplex formulation. Therapeutic effect was confirmed by the suppressed expression of mutant K-Ras gene at mRNA level. Cell viability studies demonstrated that the d-dot/PAH nanoplex formulation is highly biocompatible even at concentration as high as 160 $\mu g\ mL^{-1}$. This indicate that the d-dots can be served as a promising candidate for biomedical applications, although long term *in vitro* tests and *in vivo* experiments are required for further confirmation. The large surface area of the amine-terminated nanoplex presents plenty of opportunities for further bio-functionalization while maintaining a high siRNA loading efficiency[36]. As an example, we demonstrated that the nanoplexes can be functionalized with folic acid for receptor-mediated cancer cell targeting and gene delivery. We envision that the developed d-dot nanoplex formulation will serve as a good platform in developing and optimizing the next generation nanoplex for targeted gene therapy of pancreatic cancer in vivo.

Acknowledgements

The study was supported by Tier 1 Academic Research Funds (M4010360.040 RG29/10) and Tier 2 Research Grant MOE2010-T2-2-010 (4020020.040 ARC2/11) from Singapore Ministry of Education.

References

1. A. Vincent, J. Herman, R. Schulick, R. H. Hruban and M. Goggins, *Lancet*, 2011, **378**, 607-620.
2. S. M. Elbashir, J. Harborth, W. Lendeckel, A. Yalcin, K. Weber and T. Tuschl, *Nature*, 2001, **411**, 494-498.
3. A. de Fougerolles, H. P. Vornlocher, J. Maraganore and J. Lieberman, *Nature Reviews Drug Discovery*, 2007, **6**, 443-453.
4. K. A. Whitehead, R. Langer and D. G. Anderson, *Nature Reviews Drug Discovery*, 2009, **8**, 129-138.
5. R. L. Juliano, *Current Opinion in Molecular Therapeutics*, 2005, **7**, 132-136.
6. W. J. Song, J. Z. Du, T. M. Sun, P. Z. Zhang and J. Wang, *Small*, 2010, **6**, 239-246.
7. E. Y. Zhao, Z. X. Zhao, J. C. Wang, C. H. Yang, C. J. Chen, L. Y. Gao, Q. Feng, W. J. Hou, M. Y. Gao and Q. Zhang, *Nanoscale*, 2012, **4**, 5102-5109.
8. W. J. Li and F. C. Szoka, *Pharmaceutical Research*, 2007, **24**, 438-449.
9. V. P. Torchilin, in *Annual Review of Biomedical Engineering*, 2006, vol. 8, pp. 343-375.
10. J. M. Lee, T. J. Yoon and Y. S. Cho, *Biomed Research International*, 2013.
11. A. Kwok, G. A. Eggimann, J. L. Reymond, T. Darbre and F. Hollfelder, *Acs Nano*, 2013, **7**, 4668-4682.
12. B. Pan, D. Cui, P. Xu, C. Ozkan, G. Feng, M. Ozkan, T. Huang, B. Chu, Q. Li, R. He and G. Hu, *Nanotechnology*, 2009, **20**.
13. T. Kim and T. Hyeon, *Nanotechnology*, 2014, **25**.
14. S. B. Hartono, M. Yu, W. Gu, J. Yang, E. Strounina, X. Wang, S. Qiao and C. Yu, *Nanotechnology*, 2014, **25**.
15. B. Dubertret, P. Skourides, D. J. Norris, V. Noireaux, A. H. Brivanlou and A. Libchaber, *Science*, 2002, **298**, 1759-1762.
16. X. Michalet, F. F. Pinaud, L. A. Bentolila, J. M. Tsay, S. Doose, J. J. Li, G. Sundaresan, A. M. Wu, S. S. Gambhir and S. Weiss, *Science*, 2005, **307**, 538-544.
17. I. L. Medintz, H. T. Uyeda, E. R. Goldman and H. Mattoussi, *Nature Materials*, 2005, **4**, 435-446.
18. D. R. Larson, W. R. Zipfel, R. M. Williams, S. W. Clark, M. P. Bruchez, F. W. Wise and W. W. Webb, *Science*, 2003, **300**, 1434-1436.

19. J. M. Li, M. X. Zhao, H. Su, Y. Y. Wang, C. P. Tan, L. N. Ji and Z. W. Mao, *Biomaterials*, 2011, **32**, 7978-7987.
20. P. Subramaniam, S. J. Lee, S. Shah, S. Patel, V. Starovoytov and K. B. Lee, *Advanced Materials*, 2012, **24**, 4014-4019.
21. Y. P. Ho and K. W. Leong, *Nanoscale*, 2010, **2**, 60-68.
22. A. M. Derfus, W. C. W. Chan and S. N. Bhatia, *Nano Letters*, 2004, **4**, 11-18.
23. R. Hardman, *Environmental Health Perspectives*, 2006, **114**, 165-172.
24. H. S. Choi, W. Liu, P. Misra, E. Tanaka, J. P. Zimmer, B. I. Ipe, M. G. Bawendi and J. V. Frangioni, *Nature Biotechnology*, 2007, **25**, 1165-1170.
25. R. Hu, W. C. Law, G. Lin, L. Ye, J. Liu, J. Liu, J. L. Reynolds and K. T. Yong, *Theranostics*, 2012, **2**, 723.
26. C. Kirchner, T. Liedl, S. Kudera, T. Pellegrino, A. M. Javier, H. E. Gaub, S. Stolzle, N. Fertig and W. J. Parak, *Nano Letters*, 2005, **5**, 331-338.
27. D. Zhu, X. Jiang, C. Zhao, X. Sun, J. Zhang and J.-J. Zhu, *Chemical Communications*, 2010, **46**, 5226-5228.
28. S. Guerrero, I. Casanova, L. Farre, A. Mazo, G. Capella and R. Mangues, *Cancer Research*, 2000, **60**, 6750-6756.
29. J. B. Fleming, G. L. Shen, S. E. Holloway, M. Davis and R. A. Brekken, *Molecular Cancer Research*, 2005, **3**, 413-423.
30. T. R. Brummelkamp, R. Bernards and R. Agami, *Cancer Cell*, 2002, **2**, 243-247.
31. N. Pradhan, D. M. Battaglia, Y. C. Liu and X. G. Peng, *Nano Letters*, 2007, **7**, 312-317.
32. L. Jing, K. Ding, S. Kalytchuk, Y. Wang, R. Qiao, S. V. Kershaw, A. L. Rogach and M. Gao, *Journal of Physical Chemistry C*, 2013, **117**, 18752-18761.
33. C. L. Gan, Y. P. Zhang, D. Battaglia, X. G. Peng and M. Xiao, *Applied Physics Letters*, 2008, **92**.
34. Z.-G. Yue, W. Wei, P.-P. Lv, H. Yue, L.-Y. Wang, Z.-G. Su and G.-H. Ma, *Biomacromolecules*, 2011, **12**, 2440-2446.
35. H. Yin, R. L. Kanasty, A. A. Eltoukhy, A. J. Vegas, J. R. Dorkin and D. G. Anderson, *Nat Rev Genet*, 2014, **15**, 541-555.
36. P. Zrazhevskiy, M. Sena and X. H. Gao, *Chemical Society Reviews*, 2010, **39**, 4326-4354.